

Human Recognition through Walking Styles by Multiwavelet Transform

Farhad Mohammad Kazemi
Department of Computer Science
Memorial University of Newfoundland
St. John's, NL, Canada
fmk455@mun.ca

Wolfgang Banzhaf
Department of Computer Science
Memorial University of Newfoundland
St. John's, NL, Canada

Minglun Gong
Department of Computer Science
Memorial University of Newfoundland
St. John's, NL, Canada

Abstract— Human recognition through walking styles is among the newest of biometric methods. By using this biometric, individuals can be identified, distantly, even at low visibility. Our aim is to provide such ability for a computer system. In other words, we intend to extract appropriate features through processing video images that can reflect individuals' identity. In order to set up such a system, we have used Fourier, Wavelet, and Multi-wavelet transforms. Using images from the USF dataset version 1.7, the results obtained indicate that SA4 Multi-wavelet transforms prove more efficient in extracting suitable features than Fourier and wavelet transforms, and combined with one-versus-one Support Vector Machine, they can provide a 85.7 % recognition accuracy rate. Our proposed method shows higher accuracy and precision compared to other frequency based methods.

Keywords- Human recognition, Fourier Transform, Wavelet Transform, Multiwavelet Transform

I. INTRODUCTION

Human recognition and identification is regarded nowadays as an important field of research [1-5]. In controlled locations such as banks, military bases, and even airports, it is vital that security threats are quickly discovered and that various groups of users are provided with controlled levels of accessibility [1-3, 5]. Human beings have innate physiological or behavioral features called biometrics which can be used for human recognition and identification. Physiological biometrics are determined through the direct examination and extraction of features of a certain part of the human body. Fingerprints and retina are among the most prominent biometrics of this group. Behavioral biometrics, on the other hand, are derived from studying and extracting of human behavioral characteristics. Biometrics such as the manner of pressing keys on a keyboard or walking styles, for instance, fall into this category [1, 3-6]. Walking style has significant advantages over other biometrics – in contrast to biometrics, such as retina or fingerprint recognition, it is recognizable even from long distances and is applicable to human identification. Moreover, in terrorist attacks or security breaches, criminals often cover themselves with masks, glasses, or gloves, hence making it impossible to use other biometric features such as faces.

Walking style commonly refers to the notion of how the feet are moved. Each individual performs his/her manner of walking in a repetitive, certain way. This feature is so unique

that an individual can be recognized from a long distance [2,5,7,8]. A complete walking cycle is defined as first, the legs are located next to each other; then the right foot is lifted from the ground and moved forward. When the right foot has been placed upon the ground, the left foot is raised from the ground and moved forward so that the two feet are beside each other once again. Thus, half of the walking cycle has been completed. The second half begins with the left foot moving forward and ends with the feet being placed next to each other once more [9, 10].

Walking style has more benefits compared to other biometrics – the ability to recognize from a distance, [1-6, 11, 12], being non-offensive [1,3,4,9,11,13,14], no need for high-quality images [2-4, 10], and being impossible to hide [1,2,4,13], to name a few significant ones. On the other hand, other factors may have adverse effects on human recognition through walking styles, such as drugs and alcohol [2], physical changes caused by pregnancy, accidents, illnesses affecting the feet, and losing or gaining weight [1, 9], psychological problems such as depression or fatigue, clothing, type of shoes, the ground surface, the amount of light around, carrying heavy objects, etc [1, 16-18]. In the next section, we will describe more regarding the dataset.

Yasushi Makihara et al. introduced current progress, a research background, and basic approaches for gait recognition, and two important aspects of gait recognition, the gait databases and gait feature representations in 2015. Also, several open problems of the gait recognition discussed to show future research avenues of the gait recognition [15].

II. DATASET

In the past, studies mostly focused upon the recognition of various movements made by individuals – i.e., running, walking, jogging and climbing stairs – nowadays, however, human recognition through analyzing patterns of walking styles, become an important field of research. Datasets on walking styles are smaller than datasets of other biometrics such as fingerprints and facial recognition. Most of the previous research has been done upon small datasets (fewer than 30 individuals) and indoors [2]. One of the largest existing datasets on this subject is the USF dataset at the South Florida University. This data has been obtained outdoors, so they are influenced by factors such as shadows produced by

sunlight, background movements, and shading caused by cloud movements. The reasons why we have selected Version 1.7 of the USF dataset to implement our proposed method are:

- This dataset exceeds others concerning the number of individuals it includes: CMU MOBO consists of 25 individuals, USCD 6 individuals, GEORGIA TECH 18 individuals, MIT 24 individuals, MARYLAND 55 individuals, SOUTHAMPTON 28 individuals, whereas the 1.7 version of the USF dataset includes 71 and Version 2 consists of 122 individuals.
- Since the photography was done outdoors, images were affected by factors such as shadows forming due to the sun around the bodies, other people moving in the background, shades formed by cloud movements, etc, it is more realistic compared to datasets where controlled, laboratory conditions were used.
- This dataset is unique in its variety of photographic conditions.

III. FUNDAMENTAL CONCEPTS

Fourier, Wavelet, and Multi-wavelet transforms were used in order to extract suitable characteristics from images of silhouettes which we will discuss in brief.

A. Fourier Transform

Although most signals are normally time-dimensioned, the most important data usually lie in the frequency content of the signal. The frequency spectrum of the signal shows which frequencies the signal includes. This spectrum can be derived using the Fourier transform, which breaks the signal up into a series of mixed exponential functions with various frequencies.

The Fourier transform is reversible; i.e., it allows us to alternate between the main signal in the time dimension and the Fourier transform in the frequency dimension. However, only one of the two is possible at a time – there is no time data in the frequency dimension, and vice versa. If the signal is non-stationary – i.e. its frequency content does not change with time – there will be no problem, for all frequencies will exist at all times. However, Fourier transforms are inappropriate for non-stationary signals, for time-based, and also frequency-based data. These are required simultaneously for the analysis of these signals. Thus, we must find a more reasonable way to analyze such signals [20-23].

B. Wavelet Transform

Wavelet transforms are developed Fourier transforms, and they use short waves – wavelets instead of the exponential, sine, or cosine functions used in Fourier transforms. Wavelet transforms are quite popular in frequency analyses, for they are able to display frequencies changing with locally time. These transforms have large time ranges, and vice versa in areas of low-frequency data. This ability is called multi-resolution. Thus, wavelet transforms solve the Fourier transforms problem. As Figure 2a shows, there is no frequency-based information in the time dimension, whereas 2b contains no time-based information in the frequency dimension; the

wavelet transform in 2c, on the other hand, has varying resolution.

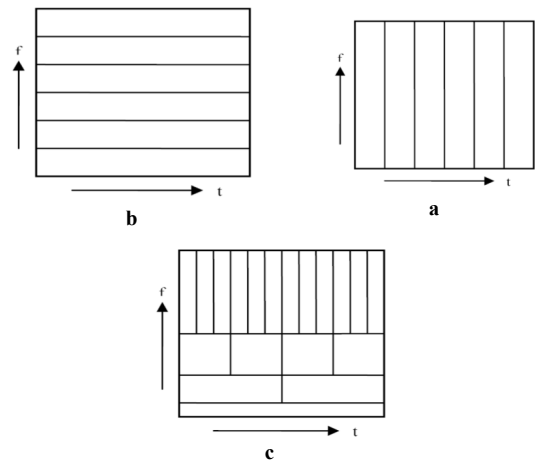


Fig 2. Time-frequency tiles: a) the time dimension, b) the frequency dimension, and c) the wavelet transform [20, 23]

The Scaling Function: $\varphi_{j,k}(x)$ functions, formed by integral transfers and the binary scaling of the real, integrable function $\varphi(x)$, can be shown as:

$$\varphi_{j,k}(x) = 2^{j/2} \varphi(2^j x - k) \quad j, k \in Z, \varphi(x) \in L^2(R) \quad (1)$$

where K shows the location of $\varphi_{j,k}(x)$ on the x axis, j is the width of $\varphi_{j,k}(x)$ and $2^{j/2}$ is its size and height. Now, with a scaling function that meets MRA's requirements, the wavelet function $\psi(x)$ can be defined so that the differences between both adjoining scaling subspaces can be covered through integral transferring and binary scaling. $\{\psi_{j,k}(x)\}$ is the set of wavelets covering W_j spaces, and is defined in Formula 2, in which $k \in Z$ shows the integral transfer and j indicates changes in function scales.

$$\psi_{j,k}(x) = 2^{j/2} \psi(2^j x - k) \quad (2)$$

Since wavelet spaces are located in spaces covered by higher-accuracy scaling functions, any wavelet function can – as its countering scaling function – be expressed as a weighted total of scaling functions with double, transferred accuracy; in other words:

$$\psi(x) = \sum_n h_\psi(n) \sqrt{2} \varphi(2x - n) \quad (3)$$

where $h_\psi(n)$ is the wavelet function coefficients vector and h_ψ is the wavelet vector. Thus, the function $f(x)$ can be displayed by expanding the scaling function in the subspace

V_{j_0} and a number of wavelet function expansions in subspaces $W_{j_0}, W_{j_0+1}, \dots$ as:

$$f(x) = \sum_k c_{j_0}(k) \phi_{j_0,k}(x) + \sum_{j=j_0}^{\infty} \sum_k d_j(k) \psi_{j,k}(x) \quad (4)$$

j_0 is the optional starting scale. $c_{j_0}(k)$ is commonly known as the estimate (or scaling coefficients), and $d_j(k)$ is the detail – or wavelet – coefficient.

-Discrete Wavelet Transforms

If the function expanding is discrete, the created coefficients thus are called DWT – discrete wavelet transforms. Therefore, DWT can be shown as:

$$W_\phi(j_0, k) = \frac{1}{\sqrt{M}} \sum_x f(x) \phi_{j_0,k}(x) \quad (5)$$

$$W_\psi(j, k) = \frac{1}{\sqrt{M}} \sum_x f(x) \psi_{j,k}(x) \quad j \geq j_0 \quad (6)$$

Reverse DWTs, on the other hand, are:

$$f(x) = \frac{1}{\sqrt{M}} \sum_k W_\phi(j_0, k) \phi_{j_0,k}(x) + \frac{1}{\sqrt{M}} \sum_{j=j_0}^{\infty} \sum_k W_\psi(j, k) \psi_{j,k}(x) \quad (7)$$

Wavelet transforms are useful for analyzing non-stationary signals. In a discrete state, filters with various cutoff frequencies are used to analyze signals in different scales. In order to separate high frequencies, signals go through several high-pass filters, whereas low-pass filters are used for lower frequencies. Signal resolution – a criterion for the total volume of data on the signal – varies with filtering operations; scales also change due to decreases in sampling and increases in the number of samples. Discrete wavelet transforms analyze signals in various frequency bands and different resolutions by means of breaking signals into sets of data estimation and data details. This transform uses scaling and wavelet functions as high-pass and low-pass filters, respectively. Breaking signals into various frequency bands is done by means of passing time-dimensioned signals through low-pass and high-pass filters repeatedly [4, 20-23].

C. Multi-wavelet Transform

Multi-wavelets are generalized versions of wavelet transforms. A wavelet transform includes a scaling function $\phi(x)$ and a wavelet function $\psi(x)$, whereas multi-wavelets consist of more than one scaling function and wavelet function; the number of scaling functions and wavelet functions in a multi-wavelet is called multiplicity. Basic multi-wavelet functions are transferred, larger versions of scaling functions $\{\phi_k(x)\}_{1 \leq k \leq M}$ and the mother wavelet function $\{\psi_k(x)\}_{1 \leq k \leq M}$ in which $M \geq 2$.

If we suppose that $\Phi(x) = (\phi_1(x), \phi_2(x), \dots, \phi_M(x))^T$ and $\Psi(x) = (\psi_1(x), \psi_2(x), \dots, \psi_M(x))^T$, then:

$$\Phi(x) = \sqrt{2} \sum_{k=0}^{L-1} H_k \Phi(2x-k) \quad (8)$$

$$\Psi(x) = \sqrt{2} \sum_{k=0}^{L-1} G_k \Psi(2x-k) \quad (9)$$

in which $\{H_k\}_{0 \leq k \leq L-1}$ and $\{G_k\}_{0 \leq k \leq L-1}$ are the filter matrices of $M \times M$ sizes. The main signal $f(t)$ must first become discrete as a vector $\{f_i\}_{1 \leq i \leq 2^j}$, in which $n = 2^j$ is the signal length. The wavelet transform receives an input sequence with the size of $n \times 1$ as its input – provided by $\{f_i\}_{1 \leq i \leq 2^j}$ – whereas multi-wavelet transforms require M input sequences of size $n \times 1$.

Multi-wavelets have benefits over wavelets. A multi-wavelet uses several scaling functions and mother wavelets, which leads to enhanced degrees of freedom when designing multi-wavelets, making it possible to have important features such as symmetry, orthogonality, and intensive support at the same time. A normal wavelet (except for the Haar wavelet) cannot enjoy all of these simultaneously [22, 24-26].

IV. THE PROPOSED METHOD

The dataset that was used in this study consists of the silhouettes extracted by the Baseline algorithm from the USF Version 1.7 dataset. Our method can be divided into three phases. Data normalization is performed in the first phase, which consists of transferring the origin of the coordinates to the center of the silhouette, changing the silhouette criterion, selecting the starting point for the silhouette's path curve, and eventually surveying the silhouette clockwise and taking 128 points as samples. The output of this phase is a vector consisting of (x, y) coordinates for these 128 points. In the second phase, Fourier, wavelet, and multi-wavelet transforms were used on this vector in order to extract the appropriate features. The feature vector obtained previously is presented to the classifiers in the third phase, the output of which is the individual's identity.

Pre-processing operations are necessary in order to turn the silhouettes created by the Version 1.7 of the Baseline algorithm into an appropriate form for recognition operations. These data need to be stable in case of transfers and changes, thus, we transferred the origin of coordinates to the center of the silhouette. Furthermore, the data must also have scaling stability. In order to create scaling stability, we normalize the size of the silhouette so that it can fit inside a single circle. The starting point for the silhouette's path curve is the point with the least distance from the top left-hand corner of the smallest rectangle of the silhouette. Having found the starting point, we surveyed the curve by means of the outer area of the silhouette's clockwise path curve. Then we took 128 samples

of the silhouette's path curve to obtain identical sample points for all silhouettes.

The individual's walking style – determined by methods used in [4, 16, 17, 45] – were mapped linearly with s frames (s frames were selected from each walking cycle); following this, pre-processing and feature extraction were performed on each frame as previously explained. The transform coefficients for each frame of a cycle make up the feature vector to be presented to the classifier, and the output of this phase is the individual's identity. Since the parameter s was set to the fixed amount of 30 in these tests, we overlook the amount of s in the following sections when we discuss feature vectors.

Although multi-layered Perceptron neural networks have incredible potential, their performance is highly affected by network architecture. An appropriate architecture for a network is defined by two main parameters: the number of hidden layers and the number of neurons in each hidden layer. On the other hand, there is no mathematical rule or formula for determining the accurate architecture of an optimized network or structure. Therefore, appropriate architecture for the network is determined empirically. We have set the following limitations for the Perceptron Neural Network architecture:

- a hidden layer
- the number of hidden neurons in the hidden layer can be calculated as:

$$s = \lfloor 2 \log_2 (m + n - 1) \rfloor \geq 2 \quad (10)$$

in which n is the number of classes, m is the input vector, and s indicates the number of neurons in the hidden layer. Further explanations on the formula can be found in [27]. Several layers of the back-propagation algorithm were used to train the Perceptron Neural Network. Moreover, we used Support Vector Machines by means of RBF kernel functions.

V. EXPERIMENTAL RESULTS

In the second phase of our method (in section VI), Fourier, Wavelet, and Multi-wavelet transforms were used in order to extract appropriate features. Moreover, the feature vector obtained previously is presented to the classifiers, in the third phase, the output of which is the individual's identity. In the following sections we analyse the results of applying Fourier, Wavelet, and Multi-wavelet transforms as feature extractors. Following this, we use four kinds of classifiers as the base of the human walking style recognition system. Each sequence for an individual consists of at least five walking cycles. We used the four first cycles in order to create training data sets, and used the remaining cycles for the test dataset.

A. Fourier Transform

The results obtained by using Fourier transforms on these 128 samples extracted from the silhouette 's path curve are presented in Table 2. These 128 points consist of x and y points as a sequence with a length of 256 coefficients. Having applied the Fourier transform to this series, a feature vector consisting of 256 coefficients was created. Through the Fourier transform, the highest recognition rate produced using a one-versus-one support vector machine is 73.3% (Table 1).

	Perceptron neural network	K-nearest neighbor	Support vector machine (one-versus-all)	Support vector machine (one-versus-one)
Recognition accuracy rates	65.4	70	67.2	73.3

The Fourier transform determines the frequency content of the signal, but it involves no time-based content; thus, two completely different signals may have the same Fourier transforms. On the other hand, individuals' walking styles and their related signals are not stationary. As a result, we require a local analysis to be able to use a combination of time-based and frequency-based analyses in order to study non-stationary signals.

B. Wavelet Transform

During recent years, wavelet transforms have become quite popular in local frequency analyses. In contrast to Fourier transforms, wavelet transforms perform signal analysis at various levels and are capable of localizing time and frequency, which makes the local features of the shape present well. From this aspect, wavelet transforms are better than Fourier transforms because they can obtain minute differences between shapes. We used Haar wavelets when implementing our experimental tests, which provide the foundation for most wavelet-based systems (see Figure 3). Their scaling and wavelet function are as follows:

$$\psi(t) = \begin{cases} 1 & 0 \leq t < 1/2 \\ -1 & 1/2 \leq t < 1 \\ 0 & \text{otherwise} \end{cases} \quad (11)$$

$$\phi(t) = \begin{cases} 1 & 0 \leq t < 1 \\ 0 & \text{otherwise} \end{cases} \quad (12)$$

The Haar wavelet has the following features:

- symmetrical scaling functions
- asymmetrical wavelet functions
- orthogonality
- intensive support (it has non-zero amounts on a short range)

Note: Only the Haar wavelet possesses such features at the same time.

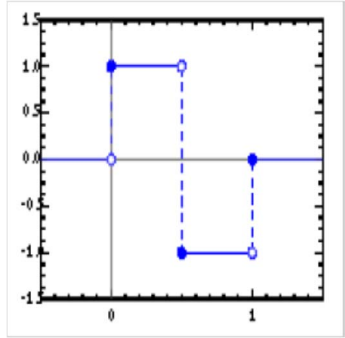


Fig. 3 The Haar wavelet

In this section, a series consisting of (x, y) coordinates relating to the 128 points of the individual's silhouette curve feed into the wavelet transform. This input sequence consisted of 256 numbers. As we have already explained, the wavelet transform analyzes this input with various numbers of coefficients. In addition, we applied the wavelet transform up to 5 levels considering the total coefficients for all 5 levels as the feature vector to make a better comparison between wavelet and Fourier transforms. The number of coefficients for the Haar transform for various levels is:

Level 1 (128), level 2 (64), level 3 (32), level 4 (16), and level 5 (8). The number of estimation coefficients in level 5 is 8. Therefore, the number of wavelet coefficients used in this step as the feature vector will be 256. Table 2 shows recognition accuracy rates using various classifiers and considering total wavelet coefficients as the feature vector.

TABLE 2. Recognition accuracy rates obtained by using the Haar wavelet

	Perceptron neural network	k-nearest neighbor	Support Vector Machine (one-versus-all)	Support Vector Machine (one-versus-one)
Recognition accuracy rate	79.3	77.8	70.4	82.5

C. Multiwavelet Transform

As we have already seen in the previous section, using wavelet coefficients with a Support vector machine (one-versus-one) classifier in the best circumstances leads to a recognition accuracy rate of 82.5 %, which is an improvement compared to the Fourier transform. Then we used Multi-wavelet transforms in order to extract appropriate features for human recognition through walking style. The main incentives for using multi-wavelet transforms are:

- Multi-wavelets provide a local frequency presentation that can reflect local features better than methods based on Fourier transform.

- Multi-wavelets supply a hierarchy multi-resolution display almost similar to the human eyesight system in multi-resolution displays.
- Multi-wavelet transforms require more than one input series. We have the coordinates for the points by taking samples of the individual's path silhouettes, which can be displayed with two vectors – x and y – and can be suitable inputs for the Multi-wavelet transform.

Due to the Multi-wavelet transform's special feature -- having two series as inputs -- a series consisting of x and y coordinates relating to the 128 points sampled from the individual's path silhouette is directly fed to the Multi-wavelet transform and the coefficients obtained will lead to the feature vector for this recognition system. We used one kind of Multi-wavelet transform here – SA4. First, we apply this transform on the 128 points mentioned above on the x and y coordinates. Thus, one matrix consisting of the coefficients created by this Multi-wavelet transform is resulted. We applied the Multi-wavelet transform up to 4 levels of analysis; the number of coefficients in various levels for this Multi-wavelet transforms is:

- The number of detail coefficients in level 1 2×64
- The number of detail coefficients in level 2 2×32
- The number of detail coefficients in level 3 2×16
- The number of detail coefficients in level 4 2×8

The number of estimation coefficients in level 4 is 8.

At first, we regard all of the existing data in the matrix formed by applying the Multi-wavelet transform as a feature vector so that we can assess the performance of this kind of Multi-wavelet combination with different classifiers. Table 3 shows the results obtained by using all Multi-wavelet coefficients and various classifiers. As seen in the table, the best results are yielded when SA4 multi-wavelets are combined and used along with one-versus-one support vector machines (85.7%).

TABLE 3. Recognition accuracy rates obtained by using all levels of analysis for SA4 Multi-wavelet coefficients

	Perceptron neural network	k-nearest neighbor	Support vector machine (one-versus-all)	Support vector machine (one-versus-one)
Recognition accuracy rate	76.4	80.2	77.5	85.7

D. A Comparison of the Performance of Fourier, Wavelet and Multi-wavelet Transforms in Feature Extraction

As displayed in Table 3, we see that Multi-wavelet transform show a better performance compared to Haar Wavelet and Fourier transforms. A comparison of the three transforms - Fourier, Wavelet, and Multi-wavelet - shows that the best combination is combining SA4 multi-wavelet and (one-versus-one) Support Vector Machine, which leads to a recognition rate of 85.7%. Thus, we see that SA4 Multi-wavelet transforms with feature vector lengths similar to those of Haar wavelet transforms lead to better recognition rates. Compared to wavelets, Multi-wavelets have advantages such as intensive support, symmetry, and orthogonality. Such features make Multi-wavelets able to work better than wavelets in many applications. Multi-wavelets are ideal for two-dimensional shapes since they can accept two or several inputs at the same time, and they lead to better results through the direct and simultaneous use of border coordinate sequences (x, y) .

VI. CONCLUSIONS AND FUTURE WORK

In this work, we have presented a model-free method for human recognition through walking styles. The empirical results obtained from USF Version 1.7 dataset imply that our proposed method has been effective. We began by performing pre-processing operations to transfer the origin of coordinates to the center of the silhouettes and normalize silhouette size. Having determined and surveyed the starting point of the silhouette's curve path, we took 128 points of this curve as samples and formed a vector with a length of 128 on x and y coordinates. In order to extract suitable features, we applied Fourier, Wavelet, and Multi-wavelet transforms to this vector and eventually presented the feature vector to the classifiers. The output of this phase is the identity of the individual. In the best circumstances, combined SA4 Multi-wavelet coefficients along with one-versus-one Support Vector Machine led to recognition rates of 85.7%.

REFERENCES

- [1] L. Wang, T. Tan, W. Hu, and H. Ning, "Automatic Gait Recognition Based on Statistical Shape Analysis," *IEEE Transactions On Image Processing*, vol. 12, No.9, .2003
- [2] M. S. Nixon and J. N. Carter, "Automatic Recognition by Gait," in *Proceedings of the IEEE*, 2006, pp. .2024-2013
- [3] S. Hong, H. Lee, K.-A. Toh, and E. Kim, "Gait Recognition Using Multi-Bipolarized Contour Vector," *SPRINGER International Journal of Control, Automation, and Systems* SPRINGER, pp. 808-799, .2009
- [4] T. Amin and D. Hatzinakos, "Wavelet analysis of cyclic human gait for recognition," in *IEEE DSP*, .2009
- [5] L. Wang, T. Tan, H. Ning, and W. Hu, "Silhouette Analysis-Based Gait Recognition for Human Identification," *IEEE Transactions On Pattern Analysis And Machine Intelligence* ,vol. 25, NO. 12, pp. 1518-1505, .2003
- [6] M. Ekinici and M. Aykut, "Improved gait recognition by multiple-projections normalization," *SPRINGER Machine Vision and Applications*, .2008
- [7] C. BenAbdelkader, R. Cutler, and L. Davisy, "Stride and Cadence as a Biometric in Automatic Person Identification and Verification," in

- Proceedings of the Fifth IEEE International Conference on Automatic Face and Gesture Recognition (FGR02)*, .2002
- [8] J.-H. Yoo and M. S. Nixon, "Feature Extraction and Selection for Recognizing Humans by Their Gait," *SPRINGER*, pp. 165-156, .2006
- [9] J. B. Hayfron-Acquah, M. S. Nixon, and J. N. Carter, "Automatic gait recognition by symmetry analysis," *ELSEVIER Pattern Recognition Letters*, .2003
- [10] A. Kale, A. Sundaresan, A. N. Rajagopalan, N. P. Cuntoor, A. K. Roy-Chowdhury, V. Krüger, and R. Chellappa, "Identification of Humans Using Gait," *IEEE Transactions On Image Processing* vol. 13, NO. 9, pp. 1173-1163, .2004
- [11] H. Lee, S. Hong, I. F. Nizami, and E. Kim, "A Noise Robust Gait Representation: Motion Energy Image," *SPRINGER International Journal of Control, Automation, and Systems* pp. 643-638, .2009
- [12] S. Yu, D. Tan, K. Huang, and T. Tan, "Reducing the Effect of Noise on Human Contour in Gait Recognition," *SPRINGER*, pp. 346-338, .2007
- [13] G. V. Veres, L. Gordon, J. N. Carter, and M. S. Nixon, "What image information is important in silhouette-based gait recognition?," in *Proceedings of the IEEE Computer Society Conference on Computer Vision and Pattern Recognition (CVPR'04)*, .2004
- [14] Y.-B. LI, T.-X. JIANG, Z.-H. QIAO, and H.-J. QIAN, "General Methods And Development Actuality Of Gait Recognition," in *Proceedings Of The 2007IEEE International Conference On Wavelet Analysis And Pattern Recognition*, Beijing, China, .2007
- [15] Makihara, Yasushi, et al. "Gait recognition: Databases, representations, and applications." *Wiley Encyclopedia of Electrical and Electronics Engineering*, 2015.
- [16] Z. Liu, "Gait-Based Human Recognition at a Distance: Performance, Covariate Impact and Solutions," in *Department of Computer Science and Engineering*. vol. Doctor of Philosophy: University of South Florida, 2004, p. .148
- [17] S. Sarkar, P. J. Phillips, Z. Liu, I. R. Vega, P. Grother, and K. W. Bowyer, "The HumanID Gait Challenge Problem: Data Sets, Performance, and Analysis," *IEEE Transactions On Pattern Analysis And Machine Intelligence*, vol. 27, NO. 2, pp. 177-162, .2005
- [18] R. T. Collins, R. Gross, and J. Shi, "Silhouette-based Human Identification from Body Shape and Gait," in *Proceedings of the Fifth IEEE International Conference on Automatic Face and Gesture Recognition (FGR'02)*, .2002
- [19] Baseline Algorithm and Performance for Gait Based Human ID Challenge Problem. 2004. Available online: <http://marathon.csee.usf.edu/GaitBaseline/>
- [20] R. C.gonzales and R. E.Woods, "Digital Image Processing," 2ed: Prentice Hall, .2002
- [21] R. Polikar, " The wavelet tutorial," Rowan University, College of Engineering, Second edition, 1999.
- [22] F. Keinert, "Wavelets and Multiwavelets," Chapman & Hall/CRC, 2004, p. .269
- [23] J. C.Goswami and A. K.Chan, "Fundamentals of wavelets , Theory, Algorithms and Applications ": A WILEY-INTERSCIENCE PUBLICATION, p. .319
- [24] S. Hongli, C. Yuanli, and Q .Zulian, "On design of multiwavelet prefilters," *ELSEVIER Applied Mathematics and Computation*, pp. 1187-1175, .2006
- [25] L. Shen, H. H. Tan, and J. Y. Tham, "Some Properties of Symmetric-Antisymmetric Orthonormal Multiwavelets," *IEEE Transactions On Signal Processing* vol. 48, NO. 7, pp. 2163-2161, .2000
- [26] X.-W. ZHANG, L. ZHU, and X.-B. ZHENG, "Study To The Image Denoising Algorithm Based On Multiwavelet Transforms," in *Proceedings Of The 2007IEEE International Conference On Wavelet Analysis And Pattern Recognition*, Beijing,China, 2007, pp. .1807-1803
- [27] G. Daqi and J. Yan, "Classification Methodologies Of Multilayer Perceptrons With Sigmoid Activation Functions," *ELSEVIER Pattern Recognition*, pp. 1469- 1482, .2005

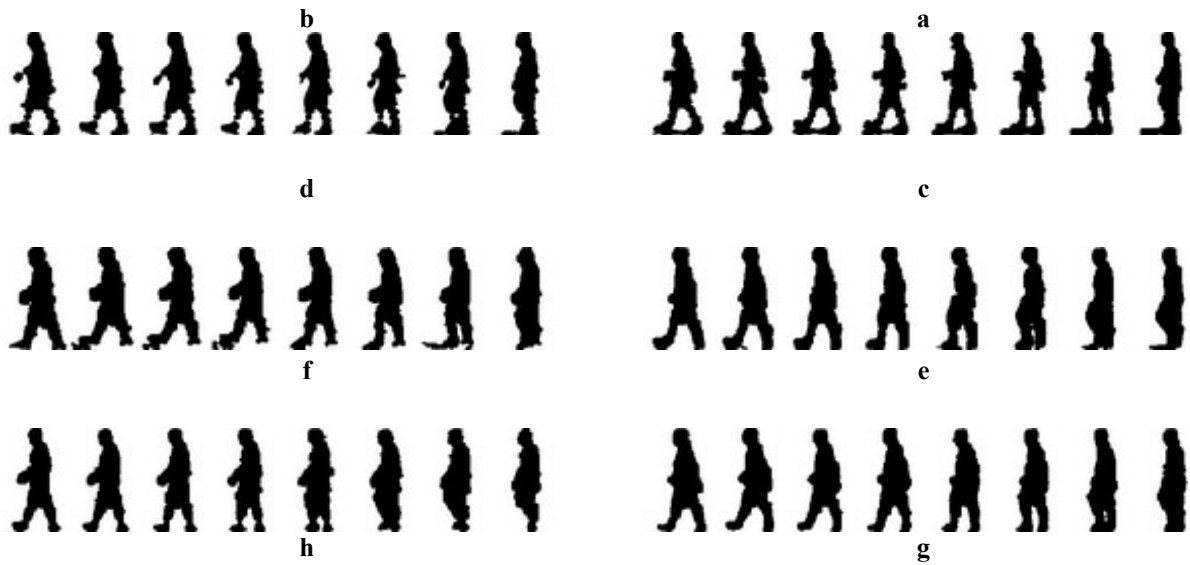


Figure 1) Samples of the silhouettes produced using the Baseline algorithm on the USF Version 1.7 dataset. These silhouettes belong to individual number 2463, who was male, 46 years old, 188 centimeters tall, weighed 102 kilograms, and more reliant on his right foot; type A shoes were sneakers, whereas type B shoes were formal and men's footwear. a) concrete surface, type A shoes, left camera b) concrete surface, type A shoes, right camera c) concrete surface, type B shoes, left camera d) concrete surface, type B shoes, right camera, e) grass surface, type A shoes, left camera f) grass surface, type A shoes, right camera g) grass surface, type B shoes, left camera h) grass surface, type B shoes, right camera [19].